



**BACHELOR OF SCIENCE IN ELECTRICAL AND ELECTRONIC
ENGINEERING**

**Low Loss Porous Core Photonic Crystal Fiber for Long Distance THz
Radiation**

Department of Electrical and Electronic Engineering

Islamic University of Technology (IUT)

Board Bazar, Gazipur-1704, Bangladesh.

November, 2016.

**Low Loss Porous Core Photonic Crystal Fiber for Long Distance THz
Radiation**

by

KM Samaun Reza

S.M. Shafi-Ur Rahman

Riasat Tanjim Hossain

A Thesis Submitted to the Academic Faculty in Partial Fulfillment of the
Requirements for the Degree of

BACHELOR OF SCIENCE

IN

ELECTRICAL AND ELECTRONIC ENGINEERING

Department of Electrical and Electronic Engineering

Islamic University of Technology (IUT)

Board Bazar, Gazipur-1704, Bangladesh.

November, 2016.

DECLARATION OF CANDIDATE

It is hereby declared that this thesis report or any part of it has not been submitted elsewhere for the award of any Degree or Diploma.

Dr. Mohammad Rakibul Islam (Supervisor)

Professor

Electrical and Electronic Engineering Department,
Islamic University of Technology (IUT), Gazipur.

KM Samaun Reza

122452

S.M. Shafi-Ur Rahman

122463

Riasat Tanjim Hossain

122466

Dedicated to our parents

ACKNOWLEDGEMENT

We would like to convey our heartiest gratitude to our supervisor Dr. Mohammad Rakibul Islam, Professor, Electrical and Electronic Engineering Department, Islamic University of Technology (IUT), Gazipur, for his encouragement and valuable advice provided to us during completion of our thesis. We couldn't have completed our research without his continuous guidance and support. We are indebted to Dr. Md. Ashrafur Hoque, Professor and Head, EEE Department, IUT for his valuable support throughout the four years of our B.Sc. course.

We are grateful to Dr. Ashik Ahmed, Assistant Professor, EEE Department, IUT for his priceless counsel on our academics.

We are thankful to Md. Saiful Islam, Assistant Professor, EEE Department, Bangladesh University (BU), for his precious advice on our research work.

We would like to thank all the faculty members and staff of the department of EEE, IUT for their inspiration and help. We would like to thank our parents for their blessings and our families and friends for having faith in us throughout the times of this thesis.

Finally, we would like to express our unparalleled gratitude to Almighty Allah for His divine blessing without which it would not have been possible to complete this thesis successfully.

KM Samaun Reza

122452

S.M. Shafi-Ur Rahman

122463

Riasat Tanjim Hossain

122466

List of Abbreviation of Technical Terms

PCF	Photonic Crystal Fiber
THz	Terahertz
EML	Effective Material Loss
MTIR	Modified Total Internal Reflection
PML	Perfectly Matched Layer
TIR	Total Internal Reflection
LC	Liquid Core
FBG	Fiber Bragg Grating
SIF	Step Index Fiber
GIF	Graded Index Fiber
LFM	Localized Function Method
FDM	Finite Difference Method
FDTD	Finite-Difference Time-Domain
FEM	Finite Element Method
FFT	Fast Fourier Transform
PMC	Perfect Magnetic Conductor
PEC	Perfect Electric Conductor

ABSTRACT

Fiber optic systems are important telecommunication infrastructure for world-wide broadband networks. Wide bandwidth signal transmission with low delay is a key requirement in present day applications. Optical fibers provide enormous and unsurpassed transmission bandwidth with negligible latency, and are now the transmission medium of choice for long distance and high data rate transmission in telecommunication networks. Our main objective is to design an optical waveguide which will be able to transmit terahertz signal into longer distances. In this thesis, two Porous-Core Photonic Crystal Fiber with ultralow Effective Material Loss (EML), high core power fraction and ultra-flattened dispersion is proposed for terahertz (THz) wave propagation. All the simulations are performed with Finite Element Modeling (FEM) package, COMSOL v4.3b. The design can be fabricated using stack and drilling method. This thesis examines effective material loss, core power fraction, modal effective area, dispersion, birefringence, confinement loss of the proposed waveguides. Characteristics analysis is done by varying the geometrical parameters. The results of the analysis are further compared with those of previous reported contributions.

Table of Contents

DECLARATION OF CANDIDATE	III
ACKNOWLEDGEMENT	V
List of Abbreviation of Technical Terms	VI
ABSTRACT	VII

CHAPTER 1

INTRODUCTION

1.1	Introduction	1
1.2	Literature Review	3
1.3	Applications of THz Radiation	5
1.4	Motivation of Work	5
1.5	Thesis Outline	6

CHAPTER 2

PHOTONIC CRYSTAL FIBER

2.1	Photonic Crystal Fibers	7
2.1.1	Features of a Photonic Crystal	8
2.2	PCF Transmitter	8
2.3	PCF Receiver	9
2.4	Porous core Photonic Crystal Fibers	10
2.5	Guiding Mechanism	11
2.6	Modal Properties of PCF	13
2.6.1	Material Absorption Loss	13

2.6.2	Porosity	13
2.6.3	Power Fraction	14
2.6.4	Confinement loss	15
2.6.5	Single-mode and Multi-mode fibers	16
2.6.6	Dispersion	17
2.6.7	Effective Area	17
2.7	Application of PCF	18
2.7.1	Dispersion Compensation	18
2.7.2	Polarization Maintaining PCF	18
2.7.3	Photonic Crystal Fibers for Sensing Applications	19
2.8	Fabrication	19

CHAPTER 3

ANALYSIS METHODS

3.1	Methodology	21
3.1.1	Effective Index Approach	21
3.1.2	Basis-Function Expansion Approach	22
3.1.3	Numerical Approach	22
3.2	Boundary Conditions	23
3.3	Background Materials	24
3.3.1	TOPAS	25
3.3.2	TEFLON	26
3.3.3	PMMA	27
3.4	Comsol Multiphysics	28
3.4.1	Design of a PCF Structure Using COMSOL	29
3.4.2	Material Define Procedure	29
3.4.3	Simulation Procedure	29

CHAPTER 4

POROUS CORE CIRCULAR PCF for THz WAVE GUIDING

4.1	Introduction	30
4.2	Design Methodology	30
4.3	Simulation and Results	32
4.4	Conclusion	39

CHAPTER 5

FUTURE WORKS AND CONCLUSION

5.1	Conclusion	40
5.2	Scope for Future Works	40

REFERENCES

APPENDIX A

A.1	MATLAB code for Calculating Single Mode Condition	46
A.2	MATLAB code for Calculating Effective Material Loss	47
A.3	MATLAB code for Calculating Core Power Fraction	47
A.4	MATLAB code for Calculating Confinement Loss	48
A.5	MATLAB code for Calculating Dispersion	49

APPENDIX B

B.1	PUBLICATIONS UNDER REVIEW	51
-----	---------------------------	----

LIST OF FIGURES

Figure No.	Figure Caption	Page No.
Fig.1.1	Structure of optical fiber	2
Fig.1.2	Terahertz frequency spectrum	3
Fig.1.3	Porous core PCF	4
Fig.2.1	Schematic of the optical frequency transfer through optical fibers	7
Fig.2.2	Periodic variations in photonic crystal fiber	8
Fig.2.3	Cross-section of (a) solid core PCF and (b) porous core PCF	11
Fig.2.4	Cross section of a porous core PCF and extended view of the core	14
Fig. 2.5	Power flow distribution of (a) low confinement loss and (b) high confinement loss designs	15
Fig. 2.6	Single-mode and multi-mode PCFs	16
Fig.2.7	A schematic representation of the stack and draw method of PCF fabrication	20
Fig.3.1	Schematic representation of a PCF	21
Fig.4.1	Cross section of the proposed fiber with an enlarged view of its core.	31
Fig.4.2	Power flow distribution of the proposed PCF for at 88% porosity	33
Fig.4.3	V parameter versus core diameter with $f=1\text{THz}$ and porosity=88%	33
Fig.4.4	V parameter versus frequency at $D_{\text{core}}=324\mu\text{m}$ and porosity=88%	34
Fig.4.5	Effective material loss as a function of core diameter at different porosities with $f=1\text{THz}$	35
Fig.4.6	Confinement loss as a function of frequency variation at $D_{\text{core}}=324\mu\text{m}$ and porosity=88%	36
Fig.4.7	Variation of EML with respect to frequency at $D_{\text{core}} = 324\mu\text{m}$ and porosity = 88%	37
Fig.4.8	Fraction of mode power through core air holes versus core diameter at different porosities at $f=1\text{THz}$	38
Fig.4.8	Fraction of mode power through air holes of the core versus frequency	38

CHAPTER 1

INTRODUCTION

1.1 Introduction

Fiber optics is a medium for carrying information from one point to another in the form of light. Unlike the copper form of transmission, fiber optics is not electrical in nature. A basic fiber optic system consists of a transmitting device that converts an electrical signal into a light signal, an optical fiber cable that carries the light, and a receiver that accepts the light signal and converts it back into an electrical signal. It was developed at 1970 firstly then it have revolutionized the telecommunication industry and have played a major role in the advent of the information age. In the developed world, optical fiber has replaced copper wire communications in core networks because of having advantages over electrical transmission. There are some basic steps which are involved in the process of communicating using fiber optics: By the use of a transmitter creating the optical signal, relaying the signal along the fiber, ensuring that the signal does not become too distorted or weak, receiving the optical signal and converting it into an electrical signal. For a large number of high-sensitivity experiments in metrology and fundamental physics, the transfer of ultra-stable frequencies between distant laboratories is an important issue for example tests of the fundamental constants stability [1].

An optical fiber's basic structure consists of three parts: the core, the cladding, and the coating or buffer. The basic structure of an optical fiber is shown in Fig.1.1. The core is like a cylindrical rod and made of dielectric materials. Dielectric materials conduct no electricity. Light propagates mainly along the core of the fiber and this core mainly made of glass. The core is described as having a radius of (a) and an index of refraction n_1 . The core is surrounded by a layer of material which is called cladding. Even light will propagate along the core only but the cladding does perform some necessary functions. The cladding layer is also made of dielectric materials with an index of refraction n_2 . The index of refraction of the cladding material is less than that of the core

material. The cladding is generally made of glass or plastic. The cladding performs the following functions:

- Reduces loss of light from the core into the surrounding air.
- Reduces scattering loss at the surface of the core.
- Protects the fiber from absorbing surface contaminants.
- Adds mechanical strength.

The cladding is enclosed in an additional layer for extra protection called the coating or buffer. The coating or buffer is a layer of material which is used to protect an optical fiber from physical damage. The material used for a buffer is a type of plastic.

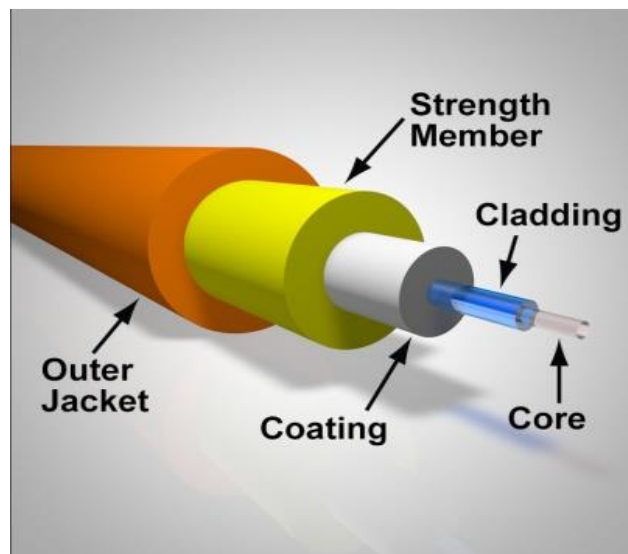


Fig: 1.1: Structure of optical fiber

The buffer is elastic in nature and prevents abrasions. The buffer also prevents the optical fiber from scattering losses which is caused by micro bends. Micro bends occur when an optical fiber is placed on a rough and distorted surface.

1.2 Literature Review

Terahertz waves (0.1 to 10 THz) have been attracting researcher's interests since the last decades due to its numerous applications in the areas of sensing [6], biotechnology [7], spectroscopy [8], imaging [9-10] and communication [12]. However, due to lack of low loss transmission waveguides, most of the THz systems depend on free space for its wave propagation. But while propagating through the free space, the propagating waves experience some undesirable problems such as tough alignment with other components, path loss, uncertain absorption loss influenced by the nature of atmosphere and many others. To overcome these free space problems, researchers proposed guided transmission medium over unguided transmission [13]. At the early stages of development, metallic waveguides and hollow dielectric metal coated tubes were introduced, but eventually disregarded due to higher loss and bulky properties [14-16]. Afterwards researchers shifted their concentration from dielectrics to polymers and towards photonic crystal fibers [17-18], polymer porous fibers [20], sub-wavelength fibers [21], hollow core Bragg fibers [19, 20] and polystyrene foams [11, 22] were introduced subsequently.

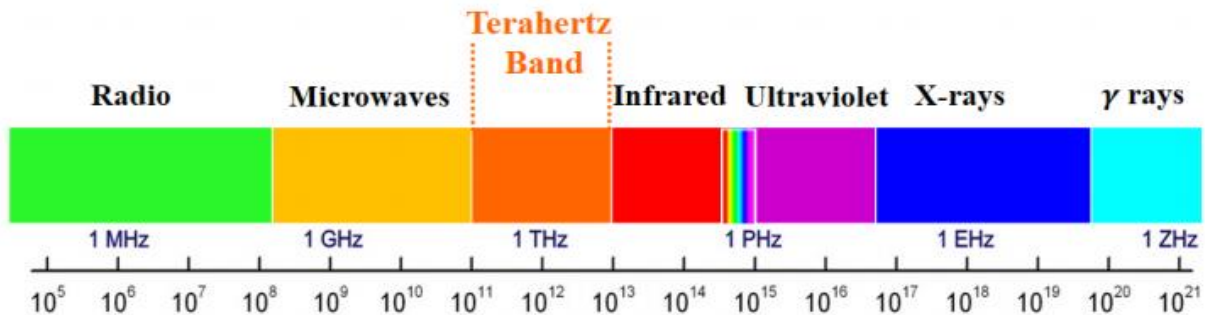


Fig: 1.2 Terahertz frequency spectrum

In the last few years, porous core Photonic Crystal Fibers (PCF) with finite number of air holes in the cladding [24-25] got much attention from all the previously proposed waveguides. In PCF, light is confined either by Modified Total Internal reflection (MTIR) or Photonic Bandgap (PBG) effect. High index core PCF guides the light by MTIR as the effective refractive index of the core is higher than that of cladding. The difference between the air core PCF and conventional PCF is the use of air holes inside the core instead of

conventional solid core. Effective Material Loss (EML) is the most important factor concerning the PCF design. EML mainly depends upon the amount of material used in the core. Higher material in the core will result higher EML. The material in the core depends on the core porosity. Porosity can be defined as the ratio of air hole area to the total cross-section area of the core. In general, higher porosity reduces the solid material inside the core, which in turn reduces the EML and vice versa [27]. In 2013, Kaijage et al. proposed a porous core photonic crystal fiber with Topas as the base material for THz wave guidance [26]. Their PCF had an EML of 0.076 cm^{-1} but ignored to analyze the dispersion and core power fraction properties of their proposed PCF.

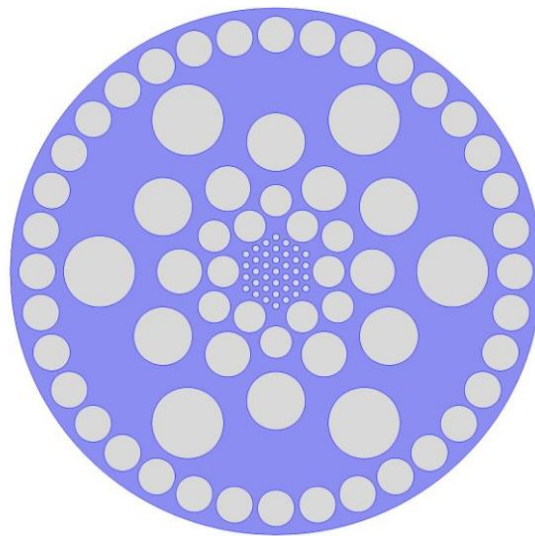


Fig: 1.3 Porous core PCF

Furthermore, Raonaq et al also reported a porous core fiber having rotated hexagonal structure in core and regular hexagonal structure in cladding [27]. They reduced the EML to 0.066 per cm and showed a core power fraction of 40%. However the EML was still higher. In addition, Rana et al. proposed another porous core fiber having octagonal structure in both core and cladding [28]. They were able to reduce the EML further to 0.058 per cm, but did not address the dispersion property. Moreover, Hasan et al. proposed a fiber having a circular structure in core and octagonal structure in cladding [29]. Without

testing the single mode operational condition of the fiber, they showed comparatively lower EML of 0.056 per cm. In recent times, Raonaq et al proposed a PCF with circular structure in both core and cladding in a more advanced work [30]. They showed a lower EML of 0.053 per cm with flattened dispersion properties. These works suggest that there is a great scope of PCF development in consideration to EML, dispersion, core power fraction and other relevant properties.

1.3 Application of THz

Numerous applications of THz radiation have been reported. They are:

- Medical diagnostics [26], [31].
- Testing of pharmaceutical drugs [26].
- Defect detection in electronic circuits [33].
- Monitoring drugs [33], [34], gas [35], explosives [36, 37], hazardous or security sensitive areas.
- Spectroscopy, imaging, sensing, security and communication [38, 40].

1.4 Motivation of Work

The variation of the structural parameters can control all propagation characteristics like effective index of the fundamental guided mode, effective mode of area and chromatic dispersion in PCF. The light in the fiber will be more confined in the core at the shorter wavelengths and the light confinement in the core can be increased by the increasing of the air filling ratio in the cladding. Structural parameter plays an important role of confining the light in the core which affects the propagation characteristics. Because of its ability to confine light in hollow cores, PCF is now finding applications in fiber-optic communications, fiber lasers, nonlinear devices, high power transmission, and highly sensitive gas sensors. Recently, researchers proposed several waveguides to transmit light into longer distances but in most cases it is seen that their obtained EML is higher with lesser core power fraction properties. In this thesis paper, EML, core power fraction, confinement loss, dispersion and effective area are thoroughly discussed.

1.5 Thesis Outline

In chapter 1, general introduction of optical fiber and previous works related to this field have been discussed. Chapter 2 includes basics of PCF, light guiding mechanisms, possible fabrication methods etc. Chapter 3 presents the analysis methods of PCF, the methods of using Comsol is also discussed in this chapter. In Chapter 4, the result and simulation of porous core circular PCF for THz wave guiding is discussed. Chapter 5 discussed about the characteristics of porous core octagonal PCF for THz wave guiding. Finally, in chapter 6, the possible future works has been discussed.

CHAPTER 2

PHOTONIC CRYSTAL FIBER

2.1 Photonic Crystal Fibers

Normally an optical fiber is a cylindrical waveguide which has a higher refractive index solid glass core in the middle of the fiber. There is another solid glass with a lower refractive index which is surrounding the core is called the cladding [40]. The index contrast between the core and the cladding traps the light inside the core and makes it propagate through the length of the fiber by the mechanism of total internal reflection (TIR) [41]. This type of optical fiber is called conventional optical fiber. On the other hand, a PCF is a single material fiber although it follows similar mechanism as conventional optical fiber. In a PCF, there are microscopic air-holes on a silica background that creates the lower refractive index cladding [42]. Generally, the core may be solid, hollow or porous. The basic distinction between conventional fiber and porous fiber is that, in a porous core the hollow core will be replaced by a number of air holes [43].

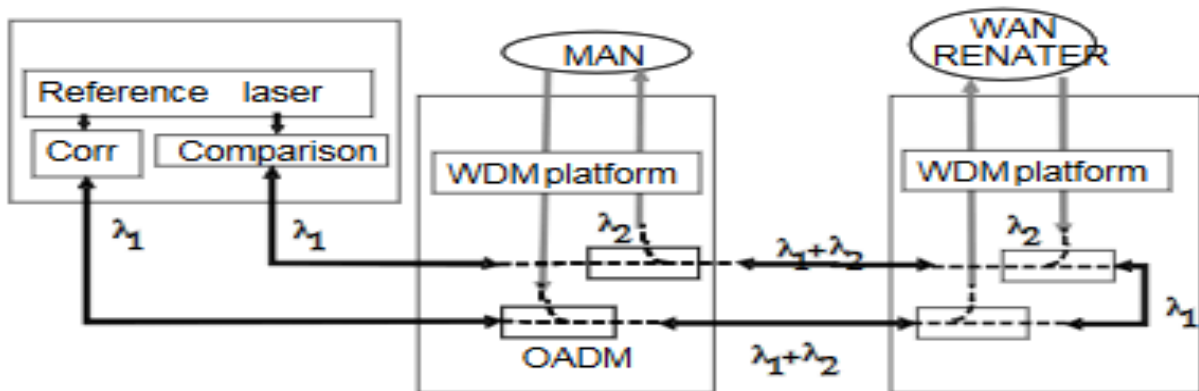


Fig: 2.1 Schematic of the optical frequency transfer through optical fibers

2.1.1 Features of a Photonic Crystal

- Made of low loss periodic dielectric medium.
- Optical analog to the electrical semiconductors.
- Able to localize light in specific areas by preventing light from propagating in certain directions-optical bandgap.
- PCF's can be of different structures. They are one dimensional, two dimensional and three dimensional. This variation is shown in Fig 2.2.

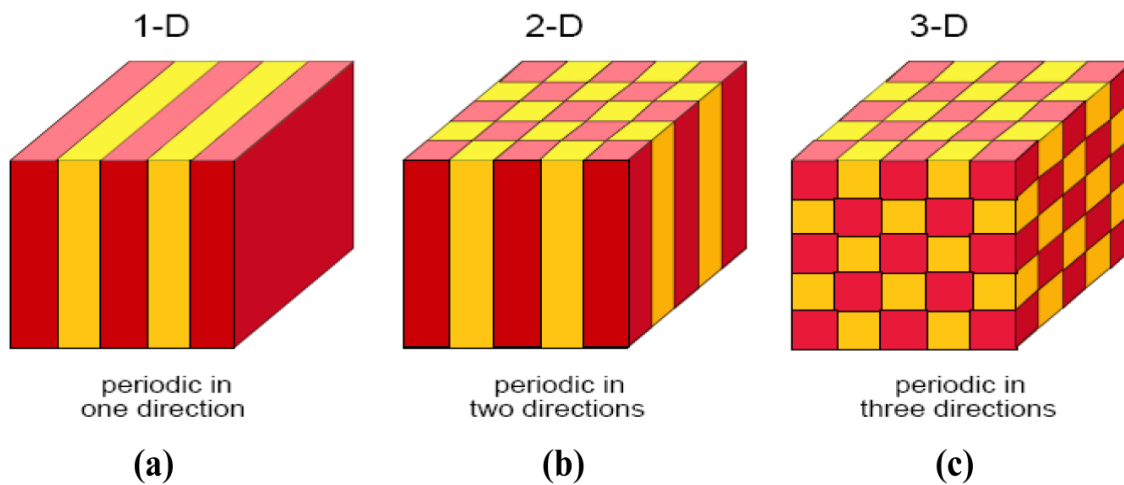


Fig 2.2. Periodic variations in photonic crystal fiber

2.2 PCF Transmitter

The most commonly-used optical transmitters are semiconductor devices such as light emitting diodes (LEDs) and laser diodes. The difference between LEDs and laser diodes is that LEDs produce incoherent light, while laser diodes produce coherent light. For use in optical communications, semiconductor optical transmitters must be designed to be compact, efficient, and reliable, while operating in an optimal wavelength range, and directly modulated at high frequencies. Early optical fiber links use amplitude modulation of an optical carrier to transmit RF and microwave frequencies [44]. In its simplest form, an LED is a forward-biased p-n junction, emitting light through spontaneous emission, a phenomenon known as electroluminescence. The emitted light is incoherent with a relatively wide spectral width of 30-60 nm. LED light transmission is also inefficient, with only about 1% of input power, or about

100 microwatts, eventually converted into launched power which has been coupled into the optical fiber. However, due to their relatively simple design, LEDs are very useful for low-cost applications. Communications LEDs are most commonly made from gallium arsenide phosphide (GaAsP) or gallium arsenide (GaAs). Because GaAsP LEDs operate at a longer wavelength than GaAs LEDs (1.3 micrometers vs. 0.81-0.87 micrometers), their output spectrum is wider by a factor of about 1.7. The large spectrum width of LEDs causes higher fiber dispersion, considerably limiting their bit rate-distance product (a common measure of usefulness). LEDs are suitable primarily for local-area-network applications with bit rates of 10-100 Mbit/s and transmission distances of a few kilometers. A semiconductor laser emits light through stimulated emission rather than spontaneous emission, which results in high output power (~100 mW) as well as other benefits related to the nature of coherent light. The output of a laser is relatively directional, allowing high coupling efficiency (~50 %) into single-mode fiber. The narrow spectral width also allows for high bit rates since it reduces the effect of chromatic dispersion. Furthermore, semiconductor lasers can be modulated directly at high frequencies because of short recombination time. Commonly used classes of semiconductor laser transmitters used in fiber optics include VCSEL (Vertical Cavity Surface Emitting Laser), Fabry-Pérot and DFB (Distributed Feed Back). Laser diodes are often directly modulated, that is the light output is controlled by a current applied directly to the device. For very high data rates or very long distance links, a laser source may be operated continuous wave, and the light modulated by an external device such as an electro-absorption modulator or Mach-Zehnder interferometer. External modulation increases the achievable link distance by eliminating laser chirp, which broadens the line width of directly-modulated lasers, increasing the chromatic dispersion in the fiber.

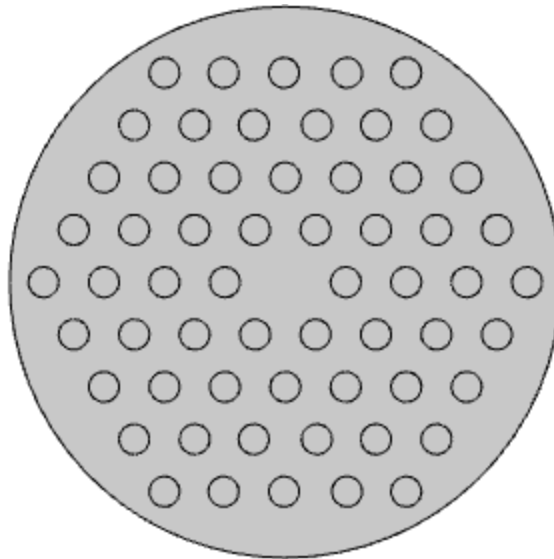
2.3 PCF Receiver

The main component of an optical receiver is a photo detector, which converts light into electricity using the photoelectric effect. The photo detector is typically a semiconductor-based photodiode. Several types of photodiodes include p-n photodiodes, p-i-n photodiodes, and avalanche photodiodes. Metal semiconductor-metal (MSM) photo detectors are also used due to their suitability for circuit integration in regenerators and wavelength-division multiplexers. Optical electrical converters are typically coupled with a trans-

impedance amplifier and a limiting amplifier to produce a digital signal in the electrical domain from the incoming optical signal, which may be attenuated and distorted while passing through the channel. Further signal processing such as clock recovery from data (CDR) performed by a phase- locked loop may also be applied before the data is passed on.

2.4 Porous core Photonic Crystal Fibers

Porous core photonic crystal fibers are similar to normal PCFs except that a large number of small air holes are used inside the core. The core formed this way is called a porous core. Generally, size of a porous core is larger than conventional PCFs. Porous core fibers have uses in low loss THz wave propagation. Inclusion of small air holes in the core reduces solid material which in turn scales down the material absorption loss. Fig. 2.3 shows the difference between a solid core and porous core PCF



(a)

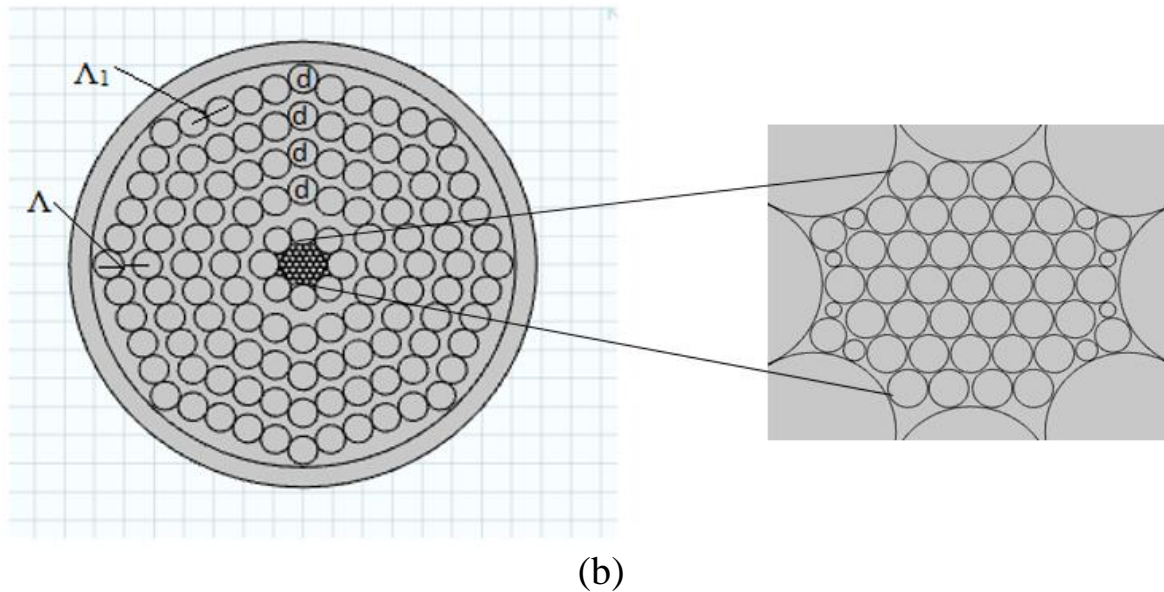


Fig 2.3. Cross-section of (a) solid core PCF and (b) porous core PCF

2.5 Guiding Mechanism

It is important to describe the mechanism or mechanisms through what the light is guided in a photonic crystal fiber. Since a PCF is a structure that usually is formed by a center core surrounding by a periodic structure (cladding), basically we can think in two possible guiding mechanism. First, we can consider the case in which the center core has an effective index of refraction than the cladding. In this case a total internal refraction kind of process occurs. We know that a ray optics picture, is not an accurate description of the electromagnetic propagation of a wave, and a wave formalism is necessary for a better understanding. The reality is that the fundamental mode is confined to the core due to the higher index of refraction, and may to leak away since the corresponding electromagnetic field are not a mode solution of Maxwell's equation for this geometry). On the other hand, higher order modes can leak away from the core (a higher field distribution in the cladding as compared with the fundamental mode). An important characteristic of PCF is that for small enough holes (air) the fiber remains single mode at all wavelength, This types of fiber is called "endlessly single mode fiber". The other guidance mechanism is a novel one and it is based in a concept that has attracted the attention of many researchers worldwide. Photonic band gap (PGB) theory has

opened a numerous application including PCF. PBG exhibit the characteristic that only certain wavelength can be transmitted. So, in a PCF the guidance process is achieved by coherent backscattering of the light into the core. Light incident upon the core-cladding interface is strongly scattered by the air-holes. For particular wavelengths the scattering process results in constructive interference of the reflected rays in the core. That guidance process enable to fabricate fiber with hollow cores (filled with air) something that it is impossible with conventional fiber (in a conventional fiber if the core is hollow, it is impossible to obtained a material with lower index of refraction than air as cladding) If the defect of the structure is realized by removing the central capillary, then guiding of an electromagnetic wave in a photonic crystal fiber can be regarded as a modified total internal reflection mechanism. The modification is due to the network of air capillaries that leak higher modes so that only one fundamental mode is carried. This is the mode with the smallest diameter, close to the size of the defect, i.e., to the lattice constant of the periodic structure. A fiber is single-mode if $d/\Lambda < 0.4$, where d is the diameter of the air channel and Λ is the crystal lattice constant. The guiding of light in a photonic crystal fiber was first demonstrated in 1996 in a solid-core fiber (solid core guidance). In a lattice of air capillaries, the central one was replaced by a rod. If the central defect is realized by inserting a central air capillary, which has a diameter different than other capillaries (usually bigger), then we can obtain a photonic band-gap (PBG). Light guidance is then an analogue of a mechanism known in solid state physics as the electron conduction mechanism in materials with an energy-band structure. In 1997 the guiding of light in an air defect was demonstrated (hollow core PGB guidance). A few central capillaries were removed from a hexagonal lattice leaving a large hole filled with air. Periodically distributed air cores can form an artificial 2D photonic crystal structure with lattice constant similar to the wavelength of light. In the 2D crystal structures photonic band-gaps exist that prevent propagation of light with a certain range of frequencies. If periodicity of the structure is broken with a defect (lack of air cores or large air core) a special region with optical properties different from the photonic crystal is created. The defect region can support modes with frequencies falling inside photonic band-gap, which prevent them from penetration of photonic crystal. The modes are strongly confined to the defects and guided along them through the fiber. Since photonic band-gap is responsible for confinement of the light in the core,

it is not required that the defect region has a higher refractive index than the surrounding [45].

2.6 Modal Properties of PCF

There are some properties of a PCF to be discussed for PCF designing. The properties are:

2.6.1. Material Absorption Loss

Every fiber optic material has bulk material loss. Bulk material absorption loss means the loss occurred due to the optical power absorption by the solid material which is quite high in THz range. Material absorption loss is reduced by replacing the solid core with porous core. The material loss occurred in a porous core PCF is called the effective material loss (EML) which is defined by the following expression [54],

$$\alpha_{eff} = \frac{\alpha_{mode}}{\alpha_{mat}} = \frac{1}{2} \left(\frac{\epsilon_0}{\mu_0} \right)^{1/2} \frac{\int_{mat} n_{mat} |E|^2 dA}{\left| \int_{all} S_z dA \right|} \quad (2.1)$$

where, α_{mat} is the material absorption loss, n_{mat} is the refractive index of the material used, α_{mode} is the fundamental mode loss and ϵ_0 , and μ_0 are the permittivity and permeability of free space, respectively. S_z is the pointing vector of z -component and $S_z = \frac{1}{2} \vec{E} \times \vec{H} \cdot \vec{z}$ where E and H are the electric and magnetic field respectively.

2.6.2 Porosity

Porous core introduces a new parameter in PCFs named porosity. The sizes of the air holes at the core determine porosity. Porosity can be defined as the ratio of air hole area to the cross section area of the core. Large numbers of air holes in the core increase the porosity and vice versa. Fig. 2.4 shows the total core

area by the blue boundary and the air hole area by the green circles. It can be expressed as,

$$\text{Porosity} = \frac{\text{Area of air holes}}{\text{Total core area}}$$

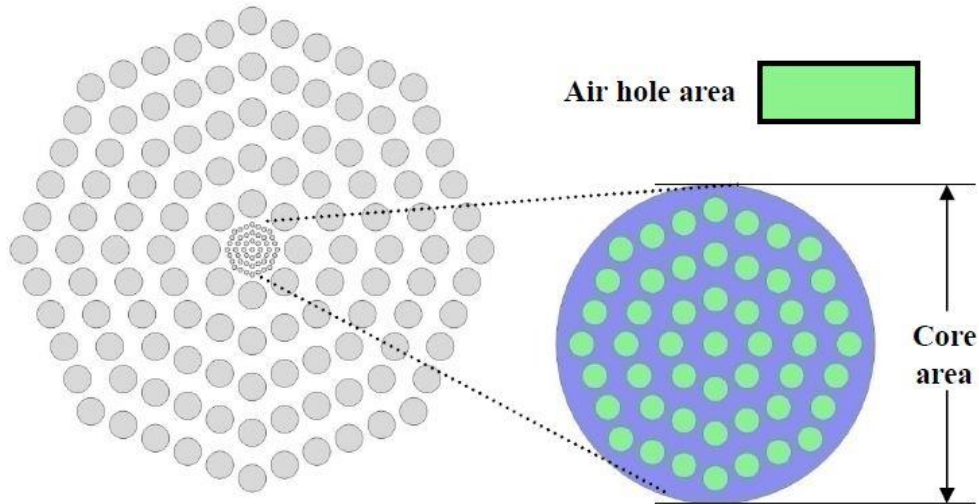


Fig 2.4. Cross section of a porous core PCF and extended view of the core

2.6.3 Power Fraction

The amount of power transmits through various regions of fiber is called power fraction of the fibers. Different regions include core air holes, cladding air holes and core background material. The sum of transmitted power through along the length of the fiber above three regions must be equal to the total power. The power flow distribution of different regions or power fraction can be estimated by the equation [54],

$$\eta' = \frac{\int_X S_z dA}{\int_{all} S_z dA} \quad (2.2)$$

Where symbol X represents the integral region which one interests.

2.6.4 Confinement Loss

Finite number of cladding air holes is the only reason of confinement loss. Some of the guided light penetrates through the cladding region due the confinement loss. Index guiding PCFs follow the same mechanism TIR as the conventional fibers and support three kinds of modes namely- the guided mode, the radiation mode, and the leaky mode. As in PCFs, the refractive index of the core and the cladding are same except that there are a finite number of air-holes in the cladding.



Fig 2.5 Power flow distribution of (a) low confinement loss (b) high confinement loss designs

The confinement loss can be obtained from the imaginary part of the complex refractive index, given by [54],

$$\alpha_{cl} = 0.8686 \frac{2\pi f}{c} \text{Im}(n_{eff}) \text{ dB/cm}$$

or

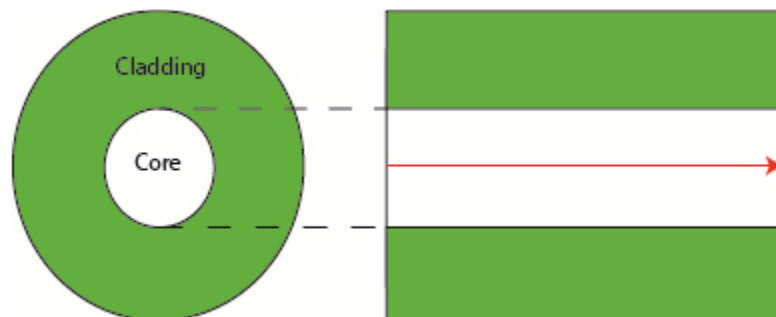
$$\alpha_{cl} = 3.7697 \frac{2\pi f}{c} \text{Im}(n_{eff}) \text{ cm}^{-1}$$

$$\text{where } 1 \text{ cm}^{-1} = 4.34 \text{ dB/cm}$$

In Eq. (2.3), f is the frequency of the light is, c the speed of the light in vacuum and $\text{Im}(n_{eff})$ the imaginary part of the refractive index of the guided mode. Fig. 2.5 (b) shows higher confinement loss than Fig. 2.5 (a) since some of the mode power spread into the cladding region.

2.6.5. Single mode and Multi-mode fibers

When the core diameter is almost equal to the wave length of the emitted light, the wave propagates along a single path. This is called the single mode operation. It supports the fundamental mode only.



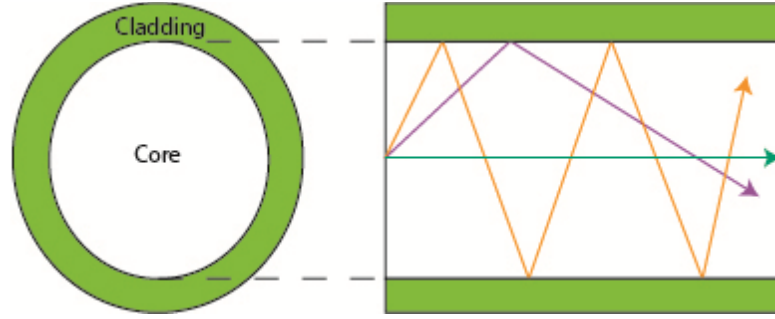


Fig 2.6. Single mode and multi-mode PCFs

When different modes exist simultaneously on the same wavelength, the operation is called multi-mode operation. Whether a fiber supports single-mode or multi-mode operation is determined by [54],

$$V = \frac{2\pi r}{c} \sqrt{n_{co}^2 - n_{cl}^2} \leq 2.405$$

Where, r is the radius of the core, c is light speed in vacuum and n_{co} and n_{cl} are the refractive indices of the fiber core and the cladding respectively. It can be deduced from

Eq. (2.4) that the value of the V -parameter must be less or equal to 2.405 for the fiber to guarantee single mode operation, otherwise not.

2.6.6 Dispersion

In fiber optic transmissions, chromatic dispersion is a term used to describe the spreading of a light pulse as it travels down a fiber when light pulses launched close together (high data rates) spread too much and result in errors and a loss of information. The chromatic dispersion $B2$ of a PCF is calculated by

$$B2 = \frac{2}{c} \frac{dn_{eff}}{d\omega} + \frac{w}{c} \frac{d^2n_{eff}}{d\omega^2} \quad (2.5)$$

Where c denotes the velocity of light in a vacuum.

2.6.7 Effective Area

The effective mode area A_{eff} , is computed using transverse electric or magnetic field vector of the whole cross sectional area of the fiber. The effective area of the of the fiber core A_{eff} is defined as [54]

$$A_{eff} = \frac{[\int I(r)rdr]^2}{[\int I^2(r)dr]^2}$$

Where $I(r) = |Et|^2$ is defined as the transverse electric field intensity distribution in the cross section of the fiber.

2.7 Application of PCF

There are several applications of PCF, some of which are started below-

2.7.1 Dispersion Compensation

A very interesting application of photonic crystal fiber is as dispersion tailoring devices. As a general rule, the bigger the dispersion compensation, the smaller the PCF length. What distinguish PCF as dispersion compensation technique compare with other method, is the fact that the range at which the compensation is made in a PCF (zero dispersion) is broad compare with the other methods. This is especially important for WDM, where compensation must be done in a broad range. The range at which compensation can be made is fundamental limited by the index contrast of the fiber. So, to increase the dispersion the index contrast must be increased, and this usually done by increasing the air-holes diameter. A typical number for the PCF dispersion is around 2000 ps-nm-1-Km-1, which means that a photonic crystal fiber can compensate 100 times its length.

2.7.2 Polarization Maintaining PCF

Birefringence in an optical fiber arises as a consequence of stresses generated in the fiber during the fabrication process. This anisotropy has an important effect in the transmission characteristics of the fiber. Birefringence can also be induced by bending and thermal effect. The net effect is the generation of different optical axes. Plane polarized light propagating along the fiber will be resolved into components along in theses axes and as they propagate at different speeds. As a result phases differences are created resulting in

elliptically polarized light. Finally, this phases mechanism cause delays in the optical signal, and this is known as polarization mode dispersion. PMD becomes important at high transmission rate. Polarization maintaining PCF is emerging as a new competitor for traditional polarization maintaining fiber. One advantage of PCF is that they remain single mode and thus can transmit polarized light in a broad range of frequencies. Also PCF has shorter beat length than common PMF which reduces bend-induced coupling between polarization states and improve the extinction rate. PCF presents, more stable temperature coefficient of birefringence. PCF's find application in sensors gyroscopes and interferometers.

2.7.3 Photonic Crystal Fibers for Sensing Applications

In PCFs, by varying the size and location of the cladding holes and/or the core the fiber transmission spectrum, mode shape, nonlinearity, dispersion, air filling fraction and birefringence, among others, can be tuned to reach values that are not achievable with conventional optical fibers. Additionally, the existence of air holes gives the possibility of light propagation in air, or alternatively provides the ability to insert liquids/gases into the air holes. This enables a well-controlled interaction between light and sample leading to new sensing applications that could not ever be considered with standard OFs. Due to PCFs diversity of features they introduce a large number of new and improved applications in the fiber optic sensing domain.

2.7.4 Fabrication

Fabrication of both PCF and conventional optical fibre requires first the creation of a macroscopic preform of the desired microscopic fibre structure. These preforms are then drawn to fibre on a fibre drawing tower in a similar manner to the fabrication of seaside rock. There are a number of ways of fabricating PCF preforms, with the most common being the stack and draw method (fig. 2.7). First, capillaries are drawn from glass tubes and then stacked in a close packed array with any solid defects (such as the core) created by the replacement of a capillary with a solid rod. This "stack" is then inserted into a tube (typically 20-25 mm in diameter), and put on a fibre drawing tower, and drawn down to the preforms (typically 1-4 mm in diameter). These performs provide a useful intermediate stage before drawing to fibre. The holes in the

preforms are generally pressurized as they are drawn to fibre. This can maintain the structure, or allow the holes to collapse or to be inflated. It is even possible to apply different pressures to different holes by inserting capillaries into them and pressurizing the capillaries; this technique has been used to make polarization-maintaining PCFs [46]. PCF preforms can also be created by drilling the desired structure into a solid rod. This technique not only limits the length of the preforms by the length of the drill bit, but also requires the silica cladding web to be thick walled in order to prevent the walls from breaking. PCFs fabricated from soft glasses such as tellurite have also been reported [47-49]. Here, the lower melting point of the glass allows preforms to be fabricated by extruding pellets of the glass through a metal die.

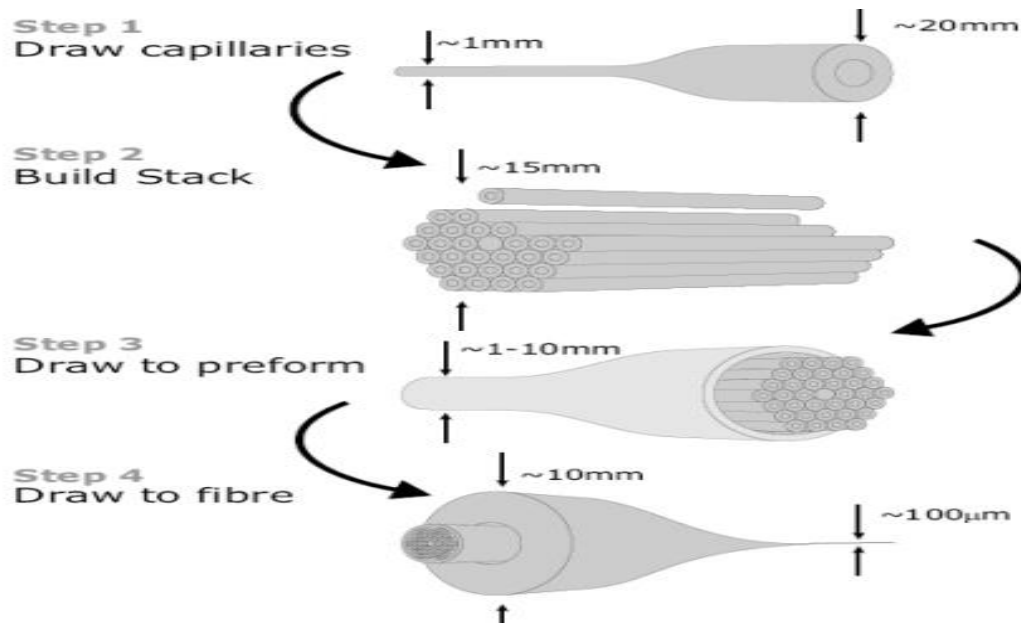


Fig 2.7: A schematic representation of the stack and draw method of PCF fabrication. First, capillaries are drawn from pure silica tubes (1) and are then stacked in a close packed array with the introduction of a defect region to form the core (2). These are drawn down to preforms (3) which are then jacketed in a silica tube and drawn to fibre (4).

CHAPTER 3 ANALYSIS METHODS

3.1 Methodology

In general three methods are utilized to analyze the structure and the properties of photonic crystal fibers.

The methods are:

- Effective Index Approach
- Basis-Function Expansion Approach
- Numerical Approach

3.1.1 Effective Index Approach

The cross section of a typical index-guiding PCF is schematically shown in Fig. 3.1, where Λ is the center-to-center distance between the holes and d is the hole diameter.

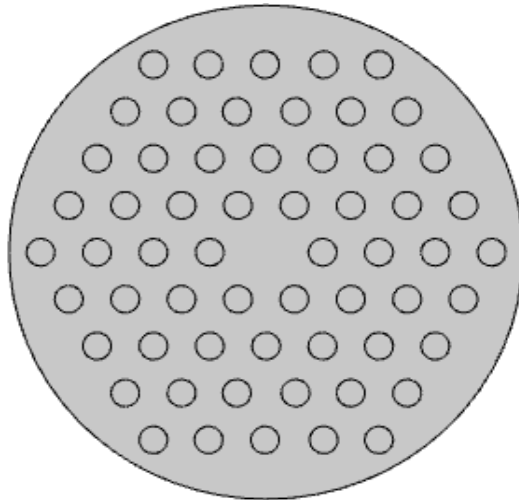


Fig.3.1. Schematic representation of a PCF

The first approach developed for PCFs was the effective index approach based on a very simple scalar model using an effective cladding index. In this model, first, an effective index for the periodically repeated hole-in-silica structure is evaluated and then the micro-structured cladding region is replaced by a uniform medium with a properly chosen effective index, resulting in an equivalent step index fiber (SIF) consisting of a core and a cladding region. Using this simple model and the well-established fiber theory, we can obtain qualitative information about PCFs with perfect hexagonal symmetry [50].

3.1.2. Basis-Function Expansion Approach

Although the effective index approach can provide good qualitative information about PCFs, this approach is unable to accurately predict modal properties such as dispersion or birefringence. These quantities depend critically on PCF geometries. An early full vector model for PCFs has been based on a modal decomposition technique using various basis functions such as sinusoidal functions, Hermit–Gaussian functions and cylindrical functions.

3.1.3 Numerical Approach

Although the basis-function expansion approach can accurately predict the modal properties such as dispersion and birefringence, it is difficult to apply it to more complicated fibers with noncircular air holes and/or longitudinally varying structures. Recently, published models utilize other direct numerical analysis techniques such as BPM, FDM , FDTD , BEM and FEM. In the FEM, instead of solving the wave equation, the corresponding functional to which a variation method is applied is set up, where the fiber cross section is divided into the so -called elements, an equivalent discretized model for each element is constructed, and then all the element contributions to the whole fiber cross section are assembled, resulting in a

matrix Eigen-value problem with nodal variables as unknowns, in contrast to the basis-function expansion approach taking expansion coefficients as unknowns. As a result, the matrices derived from the FEM and the basis-function expansion approach become sparse and dense, respectively for the characterization of longitudinally varying PCFs, the BPM is clearly the natural choice [50]. A finite element based optical mode solver is the most popular method to rigorously analyze photonic crystal fibers. Since the introduction of the photonic crystal fiber (PCF), various wave guiding structures that utilize the arrangement of micro-structured holes or thin layers have been realized. The large variety of possible hole shapes and arrangements demand the use of numerical methods that can handle arbitrary cross-sectional shapes to analyze this kind of structures. Besides, the existence of interfaces with high index-contrast between the solid host material and air holes calls for the use of the vectorial wave equation to accurately model the structure. Finite element method (FEM) is suitable for such analysis as it can handle complicated structure geometries and solve vectorial equations transparently.

3.2 Boundary Conditions

During the numerical analysis, we have considered three types of boundary conditions.

They are

- **Perfect Electric Conductor (PEC)** This boundary condition can be expressed as,

$$\mathbf{n} \cdot \mathbf{B} = 0$$

$$\mathbf{n} \times \mathbf{E} = 0 \quad (3.4)$$

Here, \mathbf{n} is the unit normal vector to the boundary. According to this condition, tangential components of \mathbf{E} and normal components of \mathbf{B} is continuous across any interface.

- **Perfect Magnetic Conductor (PMC)** This boundary condition can be expressed as,

$$n \cdot D = 0$$

$$n \times H = 0 \quad (3.5)$$

According to this condition, tangential components of H and normal components of D is continuous across any interface.

- **Perfectly Matched Layer (PML)**

A perfectly matched layer is an artificial boundary condition implying perfect absorption of incident electric field. This boundary condition is required for approximating infinite zone beyond the waveguide outer edge to a finite domain of numerical analysis. Effect of PML on numerical solutions obtained will be more prominent when confinement of field in the PCF is weak. This layer can also be utilized to find out the complex part of effective index. The PML region can be viewed as a perfect absorber with a certain magnitude of conductivity. However, the optimized conductivity is calculated from certain sets of equations. In our work, we have considered cylindrical PML available in the COMSOL software.

3.3 Background Materials

Most commonly used background materials are:

- TOPAS
- Teflon
- PMMA

3.3.1. TOPAS

Topas is the trade name for Topas Advanced Polymers cyclic olefin copolymers (COC). The Topas COC family, in contrast to the partially crystalline polyolefin PE and PP, consists of amorphous, transparent copolymers based on cyclic olefins and linear olefins. Cyclic olefin copolymers are a new class of polymeric materials with property profiles which can be varied over a wide range during polymerization.

These new materials exhibit a unique combination of properties of which can be customized by varying the chemical structure of the copolymer. Performance benefits include:

- Low density
- High transparency
- Low birefringence
- Extremely low water absorption
- Excellent water vapour barrier properties
- Variable heat deflection temperature up to 170 °C
- High rigidity, strength and hardness
- Very good blood compatibility
- Excellent biocompatibility
- Very good resistance to acids and alkalis
- Very good electrical insulating properties
- Very good melt process-ability/flow-ability

Topas COC resins are suitable for the production of transparent moldings for use in optical data storage, optics, e.g. Lenses, sensors, and industrial products e.g. in the construction and lighting sectors. These materials are also of particular interest for primary packaging of pharmaceuticals, medical devices and diagnostic disposables. (Co)-extruded films made from Topas (COC) offer opportunities in blister packaging, shrink sleeves, shrink films and stand-up pouches. New applications have been developed for blends of Topas COC, with a variety of polyolefins.

Key properties and uses of TOPAS COC resin grades include:

- **Purity:** from direct drug contact to food packaging films, TOPAS COC medical plastics have very broad global regulatory approval.
- **Glass-Clear:** lightweight optics, sparkling films, glass-like healthcare containers and high performance diagnostics with UV transparency. Amorphous: heat resistance in PCR plates, packaging, sterilizable devices and more, plus thermo formability. Olefin: compatible blends with polyethylene, often with improved reclaim and recycle characteristics for sustainability.
- **Barrier:** resists moisture, alcohols, acids and more for product protection in foods, medicine, and electronics. In our designed work, TOPAS is used as the background material due to its unique characteristics mentioned above.

3.3.2 TEFLON

PolyTetraFluoroEthylene is a fluorocarbon-based polymer and is commonly abbreviated PTFE. The Teflon brand of PTFE is manufactured only by DuPont. Several other manufacturers make their own brands of PTFE which can often be used as substitute materials. This fluoroplastic family offers high chemical resistance, low and high temperature capability, resistance to weathering, low friction, electrical and thermal insulation, and "slipperiness". (see also Teflon PTFE and Teflon FEP & PFA Specifications) PTFE's mechanical properties are low compared to other plastics, but its properties remain at a useful level over a wide temperature range of of -100°F to +400°F Mechanical properties are often enhanced by adding fillers (see paragraph below). It has excellent thermal and electrical insulation properties and a low coefficient of friction. PTFE is very dense and cannot be melt processed it must be compressed and sintered to form useful shapes.

3.3.3 PMMA

PMMA is a linear thermoplastic polymer. PMA has a lack of methyl groups on the backbone carbon chain - its long polymer chains are thinner and smoother and can slide past each other more easily, so the material becomes softer. PMMA has high mechanical strength, high Young's modulus and low elongation at break. It does not shatter on rupture. It is one of the hardest thermoplastics and is also highly scratch resistant. It exhibits low moisture and water absorbing capacity, due to which products made have good dimensional stability. Both of these characteristics increase as the temperature rises.

PMMA is one of the polymers that is most resistant to direct sunshine exposure. Its strength characteristics exhibit fairly small variations under the effect of UV- radiation, as well as in the presence of ozone. These properties of PMMA make it suitable for products intended for long open-air operation. The low water absorption capacity of PMMA makes it very suitable for electrical engineering purposes. Its dielectric properties are very good, but polystyrene and LDPE are superior to it. Its resistivity depends on the ambient temperature and relative humidity. The dielectric constant, as well as the loss tangent, depends on the temperature, the relative humidity of air and the frequency.

PMMA exhibits very good optical properties – it transmits more light (up to 93% of visible light) than glass. Combined with its good degree of compatibility with human tissue, it can be used for replacement intraocular lenses or for contact lenses. Unlike glass, PMMA does not filter ultraviolet light. It transmits UV light down to 300 nm and allows infrared light of up to 2800 nm to pass. PMMA is an economical, versatile general-purpose material. It is available in extruded and/or cast material in sheet, rod and tube forms, as well as custom profiles.

Various types of acrylics are used in a wide variety of fields and applications, including:

- **Optics:** Dust covers for hi-fi equipment, sunglasses, watch glasses, lenses, magnifying glasses.
- **Vehicles:** Rear lights, indicators, tachometer covers, warning triangles.
- **Electrical engineering:** Lamp covers, switch parts, dials, control buttons.
- **Office equipment:** Writing and drawing instruments, pens.
- **Medicine:** Packaging for tablets, pills, capsules, suppositories, urine containers, and sterilisable equipment.
- **Others:** Leaflet dispensers, shatter-resistant glazing, shower cubicles, transparent pipelines, illuminated signs, toys

3.4. Comsol Mutiphysics

COMSOL Multiphysics is a finite element analysis, solver and simulation software / FEA software package for various physics and engineering applications, especially coupled phenomena, or multiphysics. The package is cross-platform (Windows, Mac, Linux). In addition to conventional physics-based user interfaces, COMSOL Multiphysics also allows entering coupled systems of partial differential equations(PDEs). The PDEs can be entered directly or using the so-called weak form.

3.4.1 Design of a PCF Structure Using COMSOL

The following steps need to be followed first to start the design of the optical waveguide.

The steps are:

Select 2D>Radio Frequency>Electromagnetic Waves frequency domain>Mode

Analysis>Set the Length Unit to μm . The software will get opened.

To design the structure of a PCF, first set it at appropriate modal analysis, then draw the structure of PCF and give input for geometrical properties, initialize mesh and then solve the structure. The procedure for this work is given below.

- First a circular air hole is taken regarding to the circular geometry.
- Regarding the geometry the right side of the first ring was drawn.
- Mirror was used to complete the ring.
- In this way all the rings were drawn and completed the structure.
- At last part of the design PML was defined which about 10% of the fiber radius .

3.4.2 Material Define Procedure

The materials are defined using their values of refractive indexes. For TOPAS, the refractive index is 1.53 and for air the refractive index is 1.00. Also, the values of relative permittivity and relative permeability of the materials are also defined.

3.4.3 Simulation Procedure

To do simulation, the following steps should need to be followed.

- Click Study 1 in the Comsol window
- Click Step 1: Mode Analysis
- Mode analysis window will open
- Set the desired number of modes =10
- Set transform equal to effective mode index
- Vary the search for mode around from 1.00 and upto around 1.50
- Set the mode analysis frequency equal to f .

Chapter 4

POROUS CORE OCTAGONAL PCF for THz WAVE GUIDING

4.1 Introduction

In this letter a porous-core octagonally structured porous cladding photonic crystal fiber for low-loss terahertz (THz) wave guiding has been designed and analyzed. Much of attention is given to the geometries of the fibre to increase the fraction of power transmitted through core air. To investigate the transmission characteristics, perfectly matched layer (PML) is used in the outer boundary of the PCF. At an operating frequency $f = 1\text{THz}$, this design exhibits a low effective material loss of 0.046cm^{-1} at the power fraction of 42.4% with 88% porosity. Properties like: confinement loss, the power fraction of the core air holes, responses of the effective material loss, and power fraction with respect to frequency have been reported and well discussed. The design can be fabricated easily using stack and draw method and be used in potential applications in the THz region.

4.2 Methodology

The cross section of the proposed design is shown in fig-1. The air holes of the core and cladding of the proposed fiber are arranged in octagonal and rotate hexa hybrid structure respectively which accumulated 49 air holes with different radii.

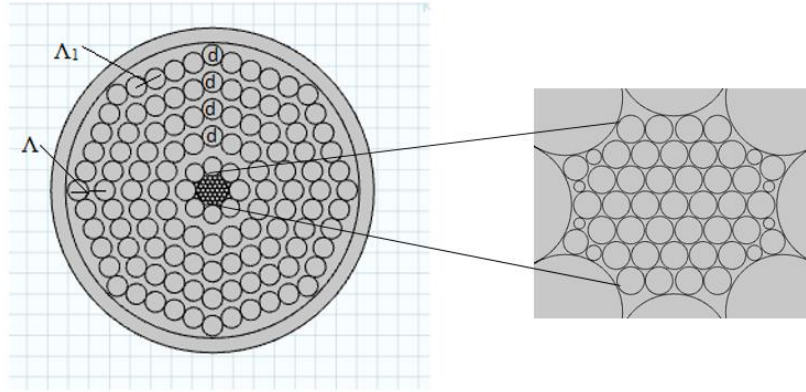


Fig.4.1. Cross section of the proposed fiber with an enlarged view of its core

Octagonally designed cladding has facilitated the model with 1.32 times more air holes in compare to a hexagonal structure with the same number of layers. 5 rings of air holes in the cladding has increased the confinement properties decreasing the material absorption loss.

Since, air holes in the core operate as low index discontinuities and dry air is transparent in THz frequency band; with the increase in number of core air holes the effective material loss decreases. Thus rotate hexa core has been considered as it has accumulated 49 air holes in the core.

The spacing between air-holes on the adjacent ring of the porous core is denoted by Λ_c and that of the cladding by Λ_1 . They are related to Λ by $\Lambda_1=0.75 \Lambda$ and $\Lambda_c= \Lambda/7.5$ respectively. The air filling fraction (AFF) is usually represented by d/Λ where d represents the diameter of the air holes. The value was fixed at 0.75 throughout the whole numerical analysis. As higher air filling fraction (AFF) increases the core confinement reducing the Effective Material Loss (EML), AFF has been kept constant. AFF in the core diameter $D_{core}=2(\Lambda-d/2)$ is variable and is mostly determined by the core porosity which is defined as the ratio of the air hole area to the cross section area of the

core. Throughout the analytical process porosity, frequency and core diameter have been varied with a keen consideration to single mode condition.

Cyclic-olefin copolymer, TOPAS has been as the background material because of its certain properties like: (1) Lower material absorption loss which is about 0.2 cm^{-1} at $f= 1\text{THz}$ (2) Constant refractive index $n=1.53$ in the range of 0.1-1.5THz [16] (3) it is not an absorber water vapor [28]. Besides, the material absorption loss of TOPAS is much less in compare to Teflon or PMMA. This particular refractive index has resulted to almost zero dispersion.

4.3 Simulation and Result

The key propagating properties of the proposed PCF were evaluated using COMSOL Multiphysics version 4.3b. A circular perfectly matched layer (PML) has been considered. The layer is about 9% of the total radius of the whole fiber and has been used outside the computation domain for obtaining accuracy in the calculation of leakage loss. The power flow distribution provided in fig-2 with the core porosity of 88% establishes the fact that light is well confined inside the core fiber.

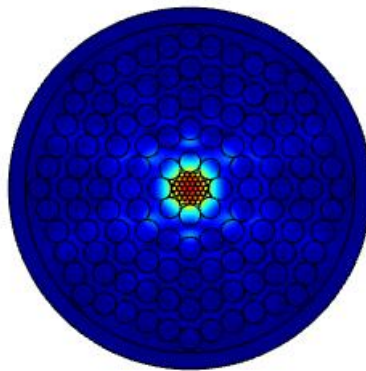


Fig.4.2. Power flow distribution of the proposed PCF at 88% porosity

It is advised to ensure that the single mode condition of the proposed fiber is not hampered with the modification of core diameter and frequency. Single

mode properties were carefully analyzed focusing on this idea. Normalized frequency or V-parameter can be calculated by [19]

$$V = \frac{2\pi r f}{c} \sqrt{n_{co}^2 - n_{cl}^2} \leq 2.405 \quad (1)$$

Where, r is defined as the core radius, c is the speed of light in vacuum, n_{co} and n_{cl} are the refractive indices of core and cladding respectively. Single mode condition is ensured when the normalized frequency V is equal to or less than 2.405. The refractive index of air is 1 [27] thus it is advantageous in assuming $n_{cl} = 1$ as the cladding consists of numerous numbers of air holes. The core refractive index n_{co} is considered to be effective refractive index (n_{eff}) because of the porous core

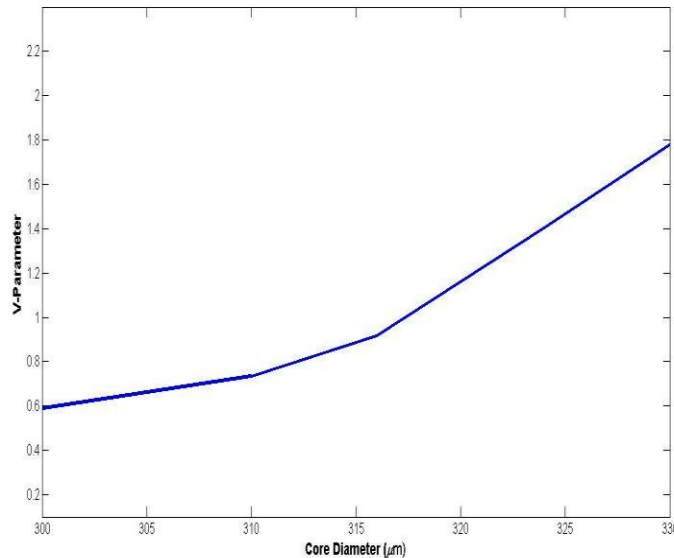


Fig.4.3. V parameter versus core diameter with $f=1$ THz and porosity=88%

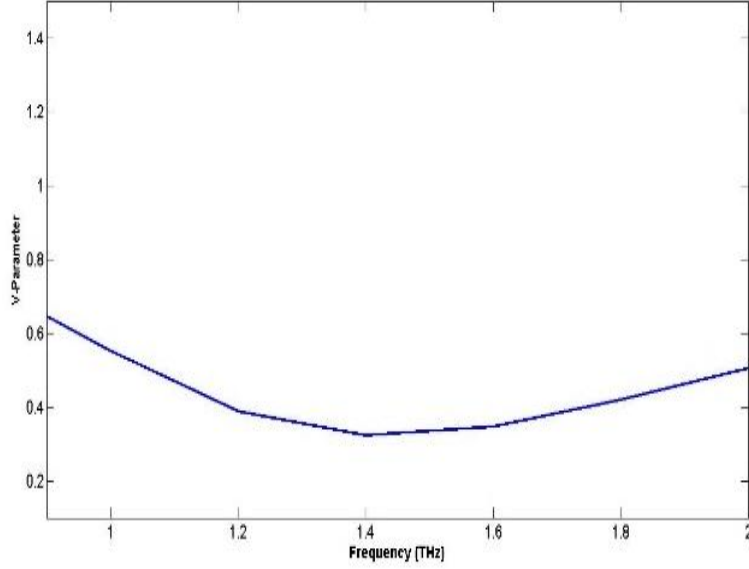


Fig.4.4. V parameter versus frequency at $D_{\text{core}}=324\mu\text{m}$ and porosity=88%.

Fig.3 and Fig.4 shows the variation of normalized frequency V with respect to different values of core diameter and frequency f. Fig 3 resembles V parameter increases with the increase of core diameter.

For designing an efficient THz waveguide, two loss properties must be considered. They are: (1) Effective material loss (2) confinement loss. The aim of the researchers from the preliminary stage was to reduce the effective material loss significantly. The effective material loss especially for PCF is often calculated by [19],

$$\alpha_{\text{eff}} = \sqrt{\frac{\epsilon_0}{\mu_0}} \left(\frac{\int_{\text{mat}} n_{\text{mat}} |E|^2 \alpha_{\text{mat}} dA}{|\int_{\text{all}} S_z dA|} \right) \quad (2)$$

Where, ϵ_0 and μ_0 are the relative permittivity and permeability in vacuum respectively, α_{mat} represents the bulk material absorption loss, n_{mat} is defined as the refractive index of Topas, E is the modal electric field and S_z is the z component of the pointing vector ($S_z = \frac{1}{2}(\mathbf{E} \times \mathbf{H}) \cdot \mathbf{z}$), here E and H are the electric and magnetic fields respectively.

When the porosity decreases the EML also decreases as the core material decreases. Fig.5 highlights the facts that, for the same porosity values there is a significant change of EML when the core diameter varies.

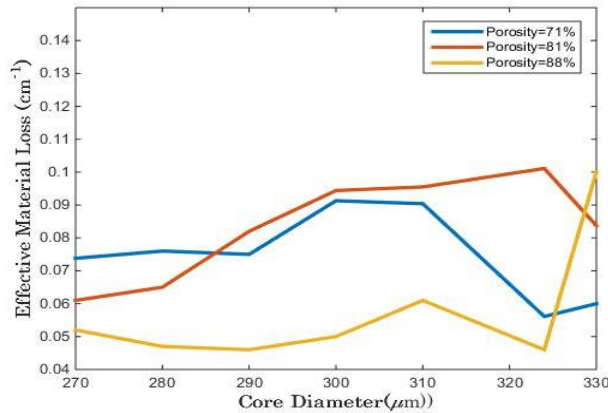


Fig.4.5. Effective material loss as a function of core diameter at different porosities with $f=1.01\text{THz}$.

Considering all these factors, EML of 0.0461 cm^{-1} at core diameter of $324\mu\text{m}$ and frequency of 1 THz is found to be the most minimized value. EML value obtained after simulation is better than the previously proposed Refs. [23-27 & 35-36].

Confinement loss is an important parameter to be considered in PCF designing. It depends upon the core porosity and the number of air holes used in cladding. It is calculated considering the imaginary part of the complex refractive index and it follows the given equation [21],

$$L_c = 8.686 \left(\frac{2\pi f}{c} \right) \text{Im}(n_{\text{eff}}) (\text{dB/m}) \quad (3)$$

Where, f is the frequency of the guiding light, c is speed of light in vacuum and $\text{Im}(n_{\text{eff}})$ symbolizes the imaginary part of the refractive index.

The confinement loss as a function of frequency is shown in Fig.6. The figure justifies that confinement loss reduces with the rise in the frequency. In the designed fiber, at $f = 1.01\text{THz}$, $D_{\text{core}} = 324\mu\text{m}$ and at 81% porosity, a confinement loss of 10^{-1}cm^{-1} is found

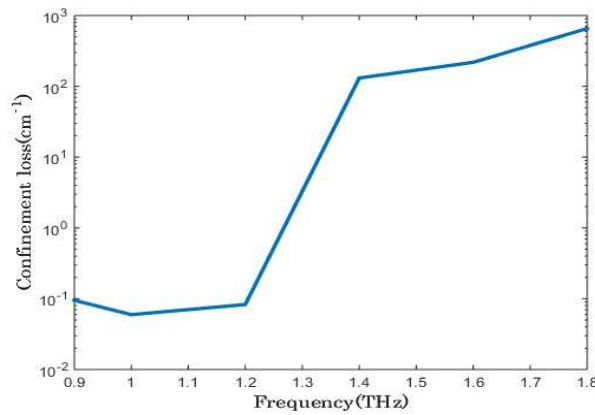


Fig.4.6.Confinement loss as a function of frequency variation at $D_{\text{core}}=324\mu\text{m}$ and porosity=88%.

Fig. 7 highlights the fact: with the increase in frequency from 1THz the EML increases. This is because, as frequency increases, the sensitivity of scattering and macro-bending losses increases.

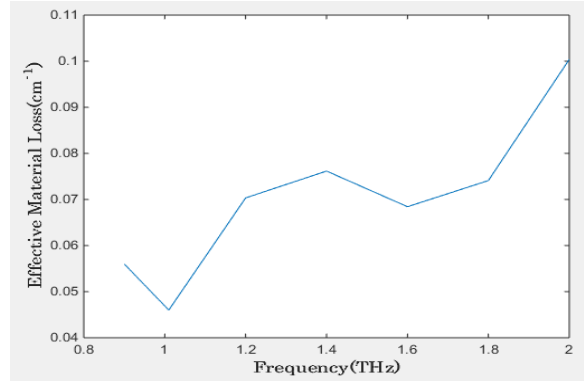


Fig.4.7. Variation of EML with respect to frequency at $D_{\text{core}} = 324\mu\text{m}$ and porosity = 88%.

The parameter which has been well explained in the paper that is the amount of mode power propagation throughout the core air holes. TO meet the criteria of standard PCF maximum power must pass through the core. The mode of power propagating through different regions of the fiber also known as core power fraction can be calculated by [29].

$$\eta' = \frac{\int_X S_z dA}{\int_{\text{all}} S_z dA} \quad (4)$$

Where, η' represents mode power fraction and X represents the area covered by air holes. As D_{core} increases the core power fraction decreases and the EML also increases. But the decrease in the power fraction EML decreases. Thus, optimal values for EML and power fraction are selected with the intentions to propose a superior design.

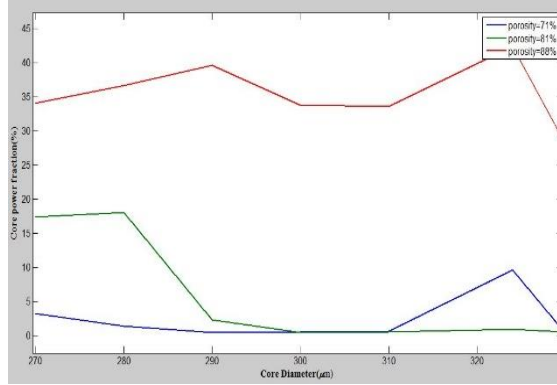


Fig.4.8. Fraction of mode power through core air holes versus core diameter at different porosities at $f=1\text{THz}$.

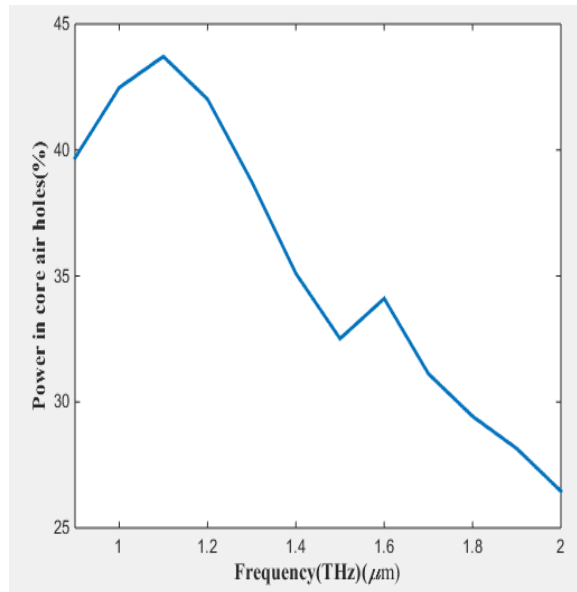


Fig.4.9. Confinement loss as a function of frequency variation at diameter of $324\ \mu\text{m}$ and porosity of 88%

In Fig.7 and Fig.8 the core power fraction at different core porosities as a function of core diameter and at different core diameter have been represented. It is observed from the same figure that, at 81% core porosity and $f= 1\text{THz}$ frequency, $D_{\text{core}} = 324\mu\text{m}$ gives 42.7% of the total power in the air core which is sufficient for THz wave guidance.

4.4 Conclusion

A comparatively simpler TOPAS based PC-OPCF with ultra-low material loss of 0.0461cm^{-1} , higher core power fraction of 42.4% has been proposed in this paper. The proposed PCF is superior to the previously proposed PCF because of its lower EML, higher core power fraction properties and simplicity in design. Therefore, if the proposed fibre is utilized properly it can be an asset for efficient, long distance and flexible transmission of THz signals because of its Ultra low material loss and higher power fraction properties.

CHAPTER 5

FUTURE WORKS AND CONCLUSION

5.1. Conclusion

In this book, porous-core PCFs with low EML and high power fraction have been presented which have promising applications in the field of THz range. In each design, core structure has been modeled carefully to increase modal power propagation through core air holes. In order to obtain an overall decent result, air filling fraction and core porosity were varied intentionally to a certain extent by considering existing fabrication techniques. A relatively simple circular PCF with rotated hexagonal porous core has been reported. The porous core made it possible to exhibit a low $EML = 0.046$ with a moderate power fraction in air core (42.4% of total power). It has been found that the octagonal structure is better than the rotated hexagonal design because the number of air holes in octagonal design is 1.32 times the hexagonal design for same number of rings.

5.2. Scope for Future Works

- High birefringence can be obtained by using dual unit based porous core and rotating core air holes at different angles.
- Effective material loss can be reduced further by increasing the porosity.
- Variation in the air holes of the core may result to the further reduction of EML.
- Increase in the number of rings in the cladding can increase the core power fraction.

REFERENCES

- [1] S.G. Karshenboim, “Fundamental physical constants: looking from different angles“, *Can. J. Phys.* 83, 767- 811, 2005.
- [2] S. M. Foreman, K. W. Holman, D. D. Hudson, D. J. Jones, and J. Ye, “Remote transfer of ultra-stable frequency references via fiber networks”, *Rev. Sci. Instrum.* 78, 021101, 2007.
- [3] C. Daussy, O. Lopez, A. Amy-Klein, A. Goncharov , M. Guine t, C. Chardonnet, F. Narbonneau, M. Lours, D. Chambon, S. Bize, A. Clairon, G. Santarelli, M.E. Tobar and A.N. Luiten, “Long -Distance Frequency Dissemination with a Resolution of 10⁻¹⁷”, *Phys. Rev. Lett.* 94, 203904, 2005.
- [4] Alwayn, Vivek, *Fiber-Optic Technologies*. Cisco Systems, 12-31, 2006.
- [5] S. M. Foreman, K. W. Holman, D. D. Hudson, D. J. Jones, and J. Ye, “Remote transfer of ultra-stable frequency references via fiber networks”, *Rev. Sci. Instrum.* 78, 021101, 2007.
- [6] R. H. Jacobsen, D. M. Mittleman and M. C. Nuss “Chemical recognition of gases and gas mixtures with terahertz waves,” *Opt Lett.*, vol. 21, no.24, pp. 2011-2013, 1996.
- [7] M. Nagel et al. “Integrated THz technology for label-free genetic diagnostics,” *Appl. Phys. Lett.*, vol. 80, no. 1, pp. 154–156, Jan. 2002,
- [8] J. Q. Zhang and D. Grischkowsky “Waveguide terahertz time-domain spectroscopy of nanometer water layers,” *Opt Lett.*, 29, no.14, pp.1617-1619, 2004.
- [9] W. L. Chan et al. “Imaging with terahertz radiation,” *Rep. Progr. Phys.*, vol. 70, no. 8, pp. 1325–1379, Aug. 2007.
- [10] D. M. Mittleman et al. “Recent advances in terahertz imaging,” *Appl. Phys. B.*, vol. 68, no. 6, pp. 1085–1094, Jun. 1999.
- [11] H. T. Chen et al. “Terahertz imaging with nanometer resolution,” *Appl. Phys. Lett.*, vol. 83,no. 15, pp. 3009–3011, Oct 2003.
- [12] L. Moller, John Federici, Alexander Sinyukov, Chongjin Xie and Hee Chuan Lim. “Data encoding on terahertz signals for

- communication and sensing,” *Optics. Lett.*, vol. 33, no. 4, pp. 393–395, Feb. 2008.
- [13] Bora Ung, Anna Mazhorova, Alexandre Dupuis, Mathieu Rozé, and Maksim Skorobogatiy “Polymer micro-structured optical fibers for terahertz wave guiding” *Opt. Exp.*, vol. 19, no. 26, pp. B848–B861, Dec. 2011.
- [14] Kanglin Wang & Daniel M. Mittleman. “Metal wires for terahertz wave guiding,” *Nature.*, vol.432,no.7015,pp. 376–379. 2004.
- [15] G. Gallot “Terahertz waveguides,” *J. Opt. Soc. Amer. B.*, vol. no.5,pp.851–863.2000.
- [16] Bradley Bowden, James A. Harrington and Oleg Mitrofanov “Silver/polystyrene-coated hollow glass waveguides for the transmission of terahertz radiation,” *Opt. Lett.*, Vol.32, no.20, pp. 2945–2947. 2007.
- [17] AHB Ghasemi “Localized modes in a defect less photonic crystal waveguide at terahertz frequencies,” *Opt. Lett.*, vol. 37, no. 13, pp. 2727–2729, Jul. 2012.
- [18] K. Nielsen “Bendable, low-loss Topas fibers for the terahertz frequency range,” *Opt. Exp.*, vol. 17, no. 10, pp. 8592–8601, May 2009.
- [19] M. Skorobogatiy and A. Dupuis “Ferroelectric all-polymer hollow Bragg fibers for terahertz guidance,” *Appl. Phys. Lett.*, vol. 90, no. 11, pp. 113514-1–113514-3, Mar, 2007.
- [20] Shaghik Atakaramians, Shahraam Afshar V., Bernd M. Fischer, Derek Abbott, and Tanya M. Monro “Porous fibers: A novel approach to low loss THz waveguides” *Opt. Exp.*, vol. 16, no. 12, pp. 8845–8854, Jun. 2008.
- [21] Chen LJ, Chen HW, Kao TF, Lu JY and Sun CK. “Low-loss sub-wavelength plastic fiber for terahertz wave guiding,” *Opt. Lett.*, vol. 31, no. 3, pp. 308–310, Feb. 2006.
- [22] Guozhong Zhao, Maarten ter Mors, Tom Wenckebach, and Paul C. M. Planken. “Terahertz dielectric properties of polystyrene foam,” *J. Opt. Soc. Amer.B.*, vol.19 , no 6, pp.1476–1479, 2002 .
- [23] Ja-Yu Lu, Chin-Ping Yu, Hung-Chung Chang, Hung-Wen Chen, Yu-Tai Li, CiLing Pan and Chi-Kuang Sun. “Terahertz air-core

- microstructure fiber,” *Appl. Phys. Lett.*, Vol.92, no. 6, pp. 064105-1064105-3, 2008.
- [24] MFO Hameed and SSA Obayya. “Polarization splitter based on soft glass nomadic liquid crystal photonic crystal fiber.” *IEEE Photonics J.*, vol.1, no.6, pp. 265–276,2009.
- [25] Mohamed Farhat O. Hameed and Salah S. A. Obayya “Modal analysis of a novel soft glass photonic crystal fiber with liquid crystal core,” *IEEE J. Lightwave Technol.*, 30, pp. 96–102, 2012.
- [26] S. F. Kaijage, Z. Ouyang and X. Jim “Porous-core photonic crystal fiber for low loss terahertz wave guiding,” *IEEE Photon. Technol. Lett.*, vol. 25, no. 15, pp. 1454–1457, Aug. 1, 2013.
- [27] Raonaqul Islam, G.K.M. Hasanuzzaman, Md. Selim Habib ,Sohel Rana and M.A.G. Khan “Low-loss rotated porous core hexagonal single-mode fiber in THz regime,” *Optical Fiber Technol.*, Vol.24, no.23,pp. 38–43, 2015.
- [28] Sohel Rana; Golam Kibria; Md. Hasanuzzaman; Md. Samiul Habib; Shubi F. Kaijage; Raonaqul Islam “Proposal for a low loss porous core octagonal photonic crystal fiber for T-ray wave guiding,” *Optical Engineering.*, vol.53, no.11, pp.115107, November 2014.
- [29] Md.Imran Hasan, S. M. Abdur Razzak ; G. K. M. Hasanuzzaman ,and Md. Samiul Habib, “Ultra-Low Material Loss and Dispersion Flattened Fiber for THz Transmission,” *IEEE Photon. Technol. Lett.*, Vol. 26, No. 23, December 1, 2014.
- [30] Raonaqul Islam and Sohel Rana. “Dispersion flattened, low-loss porous fiber for single-mode terahertz wave guidance,” *Optical Engineering*, vol.54, no.5, pp. 055102, May 2015.
- [31] R. M. Woodward, V. P. Wallace, D. D. Arnone, E. H. Linfield, and M. Pepper, Terahertz pulsed imaging of skin cancer in the time and frequency domain, *J. Biol. Phys.*, vol. 29, no. 2/3, pp. 257–261, Jan. 2003.
- [32] C. J. Strachan, P. F. Taday, D. A. Newnham, K. C. Gordon, J. A. Zeitler, M. Pepper, and T. Rades, “Using terahertz pulsed

- spectroscopy to quantify pharmaceutical polymorphism and crystallinity”, *J Pharm. Sci.*, vol. 94, no. 4, pp. 837–846, Apr. 2005.
- [33] T. Kiwa, M. Tonouchi, M. Yamashita, and K. Kawase, “Laser terahertz-emission microscope for inspecting electrical faults in integrated circuits”, *Opt. Lett.*, vol. 28, no. 21, pp. 2058–2060, Nov. 2003.
- [34] P. U. Jepsen, D. G. Cooke, and M. Koch, “Terahertz spectroscopy and imaging Modern techniques and applications,” *Laser Photon. Rev.*, vol. 5, no. 1, pp. 124–166, Jan. 2011.
- [35] K. Kawase, Y. Ogawa, Y. Watanabe, and H. Inoue, “Non-destructive terahertz imaging of illicit drugs using spectral fingerprints,” *Opt. Exp.*, vol. 11, no. 20, pp. 2549–2554, Oct. 2003.
- [36] R. H. Jacobsen, D. M. Mittleman, and M. C. Nuss, “Chemical recognition of gases and gas mixtures with terahertz waves,” *Opt. Lett.*, vol. 21, no. 24, pp. 2011–2013, Dec. 1996.
- [37] Y. C. Shen, T. Lo, P. F. Taday, B. E. Cole, W. R. Tribe, and M. C. Kemp, “Detection and identification of explosives using terahertz pulsed spectroscopic imaging”, *Appl. Phys. Lett.*, vol. 86, no. 24, pp. 241116-1–241116-3, Jun. 2005.
- [38] H. B. Liu, Y. Chen, G. J. Bastiaans, and X. C. Zhang, “Detection and identification of explosive RDX by THz diffuse reflection spectroscopy,” *Opt. Exp.*, vol. 14, no. 1, pp. 415–423, Jan. 2006.
- [39] M. M. Awad and R. A. Cheville, “Transmission terahertz waveguide based imaging below the diffraction limit,” *Appl. Phys. Lett.*, vol. 86, no. 22, pp. 221107-221107-3, May 2005.
- [40] G. P. Agrawal, *Nonlinear Fiber Optics*, Academic Press, USA, 2nd Edition, 1995.
- [41] G. P. Agrawal, *Fiber-Optic Communication Systems*, John Wiley & Sons Inc., USA, 3rd Edition, 2002.
- [42] P. St. J. Russell, “Photonic Crystal Fibers,” *Science*, vol. 299, no. 5605, pp. 358-362, Jan. 2003.
- [43] T. Wu and C. Chao, “A novel ultra-flattened dispersion photonic crystal fiber,” *IEEE Photonics Technol. Lett.*, vol. 17, pp. 67-69, 2005.

- [44] S. M. Foreman, K. W. Holman, D. D. Hudson, D. J. Jones, and J. Ye, "Remote transfer of ultra-stable frequency references via fiber networks", *Rev. Sci. Instrum.* 78, 021101, 2007.
- [45] R. Buczynski, "Photonic Crystal Fibers," *Proceedings of the XXXIII International School of Semiconducting Compounds*, vol. 106, no. 2, January 2004
- [46] C. Xiong and W. J. Wadsworth. "Polarized super-continuum in bire-fringent photonic crystal bre pumped at 1064 nm and application to tunable visible/uv generation". *Opt. Express*, 6(4):2438-2445, 2008.
- [47] K. M. Kiang, K. Frampton, T. M. Monro, R. Moore, J. Tucknott, D. W. Hewak, D. J. Richardson, and H. N. Rutt. "Extruded single mode non-silica glass holey optical fibres". *Electronics Letters*, 38(12):546–547, 2002.
- [48] V. V. Ravi Kanth Kumar, A. K. George, J. C. Knight, and P. St. J. Russell. "Tellurite photonic crystal fiber". *Opt. Express*, 11(20):2641–2645, 2003.
- [49] V. V. Ravi Kanth Kumar, A. K. George, W. H. Reeves, J. C. Knight. St. J. Russell, F. Omenetto, and A. Taylor. "Extruded soft glass photonic crystal fiber for ultra-broad super-continuum generation". *Opt. Express*, 10(25):1520–1525, 2002.
- [50] K. Saitoh and M. Koshiba, "Numerical Analysis of Photonic Crystal Fibers," *Journal of Light wave Technology*. vol. 23, no. 11, November 2005.
- [51] N. Chen, et al. "High-birefringence, low-loss porous fiber for single-mode terahertz-wave guidance," *Appl. Opt.* vol.52, no.21, pp.5297–5302, 2013.
- [52] S. M. A. Razzak and Y. Namiyama, "Proposal for Highly Nonlinear Dispersion Flattened Octagonal Photonic Crystal Fibers," *IEEE photonics technol. lett.*, vol. 20, no. 4, pp. 249-251, Feb. 2008.
- [53] Fabrication of photonic crystal fiber, "Photonic crystal fiber science," [online], <http://www.mpl.mpg.de/en/russell/research/topics/fabrication.html> (access date : Feb. 17, 2016)

APPENDIX A

A.1. MATLAB code for Calculating Single Mode Condition:

```
clc
clear all
c=3*10^8;
f=10^12;
d=((2*pi*f)/c);
x=[0.90 0.95 1.0 1.05 1.1 1.15 1.20 1.25 1.3 1.35 1.4 1.45 1.50];
a=sqrt((abs(1.04642-2.80671e-4i)^2-1))*175*10^-6;
b=sqrt((abs(1.04872-2.21323e-4i)^2-1))*175*10^-6;
c=sqrt((abs(1.04838-2.04915e-5i)^2-1))*175*10^-6;
d1=sqrt((abs(1.05538-1.59136e-5i)^2-1))*175*10^-6;
e=sqrt((abs(1.06176-2.01952e-5i)^2-1))*175*10^-6;
f=sqrt((abs(1.06673-2.27655e-6i)^2-1))*175*10^-6;
g=sqrt((abs(1.07274-9.63059e-7i)^2-1))*175*10^-6;
h=sqrt((abs(1.07959-2.49969e-7i)^2-1))*175*10^-6;
i=sqrt((abs(1.07695-9.45225e-7i)^2-1))*175*10^-6;
j=sqrt((abs(1.08731-1.67998e-7i)^2-1))*175*10^-6;
k=sqrt((abs(1.09962-6.94153e-7i)^2-1))*175*10^-6;
l=sqrt((abs(1.10759-7.97103e-8i)^2-1))*175*10^-6;
m=sqrt((abs(1.10541-8.4102e-8i)^2-1))*175*10^-6;
v=d*[a b c d1 e f g h i j k l m ];
set(gca,'FontName','arial','FontSize',14)
```

```

plot(x,v,'linewidth',2.5);
xlabel('Frequency (THz)','FontName','arial','fontweight','b','FontSize',14);
ylabel('V-Parameter','FontName','arial','fontweight','b','FontSize',14);
axis([0.9 1.25 0.9 2.4]);

```

A.2. MATLAB code for Calculating Effective Material Loss:

```

clc
clear all
d=[0.90 0.95 1.00 1.05 1.10 1.15 1.2 1.25 1.3 1.35 1.40 1.45 1.50 ];
eml=[0.04589 0.0440567 0.04076 0.04296 0.04477 0.04613 0.04852 0.05776
0.059
0.06178 0.06351 0.06509 0.06705];
set(gca,'FontName','arial','FontSize',14)
plot(d,eml,'linewidth',2.5);
xlabel('Frequency(THz)','FontName','arial','fontweight','b','FontSize',14);
ylabel('Effective Material Loss (cm^-1)','FontName','arial','fontweight',
'b','FontSize',14);
axis([0.90,1.5,0.035 0.07]);

```

A.3. MATLAB code for Calculating Core Power Fraction:

```

clc
clear all
x = [0.90 0.95 1.00 1.05 1.10 1.15 1.2 1.25 1.3 1.35 1.40 1.45 1.50];
y1=[0.04589 0.0440567 0.04076 0.04296 0.04477 0.04613 0.04852 0.05776
0.059

```

```

0.06178 0.06351 0.06509 0.06705];
y2=100*[0.39416 0.4543 0.501 0.48858 0.4772 0.44688 0.443514 0.3988
0.3726712
0.35045 0.34789 0.33637 0.32345];
set(gca,'FontName','century','FontSize',14);
[HAX,H1,H2]=plotyy(x,y1,x,y2);
xlabel('Frequency(THz)','FontName','century','fontweight','b','FontSize',12);
ylabel(HAX(1),'EML(cm^-^1)','FontName','century',
'fontweight','b','FontSize',12);
ylabel(HAX(2),'Core power
fraction(%)','FontName','century','fontweight','b','FontSize',12);
axis([.7 1.5 0 60]);

```

A.4. MATLAB code for Calculating Confinement Loss:

```

clc
clear all
k=3*10^8;
m=(4.34*0.834*(2*pi*10^12)/k)/100;
f=[0.90 0.95 1.00 1.05 1.10 1.15 1.2 1.25 1.3 1.35 1.40 1.45 1.50];
n1=[
1.04642-2.80671e-4i
1.04872-2.21323e-4i
1.04838-2.04915e-5i
1.05538-1.59136e-5i
1.06176-2.01952e-5i

```

```

1.06673-2.27655e-6i
1.07274-9.63059e-7i
1.07959-2.49969e-7
1.07695-9.45225e-7i
1.08731-1.67998e-7i
1.09962-6.94153e-7i
1.10759-7.97103e-8i
1.10541-8.4102e-8i];
a=abs (imag(n1));
c=f.*a;
Lc1=m.*c;
Lc1= smooth(Lc1);
set(gca,'FontName','century','FontSize',12)
semilogy(f,Lc1,'linewidth',2.5);
xlabel('Frequency(THz)','FontName','century','fontweight','b','FontSize',12);
ylabel('Confinement loss(cm^-
^1)','FontName','century','fontweight','b','FontSize',12);
axis([.7 1.5 .065 .082])

```

A.5. MATLAB code for Calculating Dispersion:

```

clc;
clear all;
f=[0.90 0.95 1.00 1.05 1.10 1.15 1.2 1.25 1.3 1.35 1.40 1.45 1.50];
a=[
1.04642-2.80671e-4i

```

```

1.04872-2.21323e-4i
1.04838-2.04915e-5i
1.05538-1.59136e-5i
1.06176-2.01952e-5i
1.06673-2.27655e-6i
1.07274-9.63059e-7i
1.07959-2.49969e-7
1.07695-9.45225e-7i
1.08731-1.67998e-7i
1.09962-6.94153e-7i
1.10759-7.97103e-8i
1.10541-8.4102e-8i];
neff1=real(a);
w=2*pi*f;
c=3*10^8;
disp1=diff(neff1)./diff(w);
w1=w(1:length(w)-1);
disp2=diff(disp1)./diff(w1);
w2=w(1:length(w)-2);
disp= 10^10*(2/c)*disp1(1:length(disp1)-1)+(w2./c).*disp2;
plot(f(1:length(f)-2),disp,'linewidth',2.5);
set(gca,'FontName','arial','FontSize',14);
xlabel('Frequency (THz)','FontName','arial','fontweight','b','FontSize',14);
ylabel('B2(ps/THz/cm)','FontName','arial','fontweight','b','FontSize',14);

```

PUBLICATION UNDER REVIEW

Porous-Core single-mode Photonic Crystal Fiber for Low Loss THz Wave guidance

KM Samaun Reza, S.M. Shafiur Rahman, Riasat Tanjim, Md. Saiful Islam, Mohammad Rakibul Islam